NASA TECHNICAL NOTE

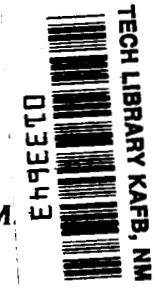

NASA TN D-6798

LIFTING-SURFACE THEORY FOR CALCULATING THE LOADING INDUCED ON A WING BY A FLAP

by Wayne Johnson

Ames Research Center

and

U.S. Army Air Mobility R&D Laboratory

Moffett Field, Calif. 94035

NATIONAL AERONAUTICS AND SPACE ADMINISTRATION • WASHINGTON, D. C. • MAY 1972

1. Report No.	2. Government Accession No.	3. Recipient's Catalog No.
NASA TN D-6798		

4. Title and Subtitle	5. Report Date
LIFTING–SURFACE THEORY FOR CALCULATING THE LOADING INDUCED ON A WING BY A FLAP	May 1972
	6. Performing Organization Code
7. Author(s)	8. Performing Organization Report No.
Wayne Johnson	A-4084
	10. Work Unit No. 760–74–07–10–00–21
9. Performing Organization Name and Address NASA Ames Research Center and U.S. Army Air Mobility R&D Laboratory Moffett Field, Calif., 94035	11. Contract or Grant No.
	13. Type of Report and Period Covered Technical Note
12. Sponsoring Agency Name and Address National Aeronautics and Space Administration Washington, D. C. 20546	14. Sponsoring Agency Code

15. Supplementary Notes

Edited by NASA Ames Research Center

16. Abstract

A method is described for using lifting-surface theory to obtain the pressure distribution on a wing with a trailing-edge flap or control surface. The loading has a logarithmic singularity at the flap edges, which may be determined directly by the method of matched asymptotic expansions. Expressions are given for the singular flap loading for various flap hinge line and side edge geometries, both for steady and unsteady flap deflection. The regular part of the flap loading must be obtained by inverting the lifting-surface-theory integral equation relating the pressure and the downwash on the wing; procedures are described to accomplish this for a general wing and flap geometry. The method is applied to several example wings, and the results are compared with experimental data. Theory and test correlate well.

17. Key Words (Suggested by Author(s))	18. Distribution Statement
Lifting-surface theory Trailing-edge flap	Unclassified – Unlimited

19. Security Classif. (of this report)	20. Security Classif. (of this page)	21. No. of Pages	22. Price*
Unclassified	Unclassified	20	$3.00

*For sale by the National Technical Information Service, Springfield, Virginia 22151

SYMBOLS

a_{nm}	coefficient of wing pressure mode
AR	aspect ratio
b	wing local semichord
c_f	ratio of local flap chord to local wing chord
c_l	section lift coefficient
C_h	hinge moment coefficient
C_L	lift coefficient
C_m	pitching-moment coefficient
f_n	chordwise pressure mode
g_f	singular part of pressure due to flap
g_m	spanwise pressure mode
$(I_f)_{ij}$	downwash at collocation point (x_i, s_j) due to flap pressure mode
$(I_{nm})_{ij}$	downwash at collocation point (x_i, s_j) due to pressure mode a_{nm}
k	wave number, $\frac{\omega}{U}$
K	kernel function relating wing pressure and downwash
$\bar{K}$	kernel function, without spanwise singularity
l, λ	normalized spanwise variable, curvilinear coordinates
M	Mach number of free stream
p	pressure at wing surface
P_{2D}	flap pressure at hinge line
P_h	flap pressure due to hinge line plus both corners
P_{Lh}	flap pressure due to hinge line plus left corner
P_{Lse}	flap pressure due to left side edge

P_{Rh}	flap pressure due to hinge line plus right corner
P_{Rse}	flap pressure due to right side edge
r_1	$\sqrt{(y - \eta)^2 + (z - \zeta)^2}$
s_{TIP}	wing semispan
s,σ	spanwise variable, curvilinear coordinates
U	free-stream velocity
v_n	downwash at wing surface
v_n^*	effective downwash at wing surface
$\bar{x}$	wing local midchord
x_c	flap hinge line
x_{LE}	wing leading edge
x_{TE}	wing trailing edge
x,ξ	chordwise variable
y_L	left side edge of flap
y_R	right side edge of flap
y_s	side edge of flap
y,η	spanwise variable
z,ζ	vertical variable
β	$\sqrt{1 - M^2}$
β_N	$\sqrt{\beta^2 \cos^2 \Lambda + \sin^2 \Lambda}$
δ_f	downward flap deflection
ϵ	half width of integration strip containing collocation point
Λ	sweep angle of flap hinge line
ρ	air density

ϕ_c	normalized flap hinge line location
ϕ,θ	normalized chordwise variable
ω	frequency

LIFTING–SURFACE THEORY FOR CALCULATING THE LOADING INDUCED ON A WING BY A FLAP

Wayne Johnson

Ames Research Center
and
U.S. Army Air Mobility Research and Development Laboratory

SUMMARY

A method is described for using lifting-surface theory to obtain the pressure distribution on a wing with a trailing-edge flap or control surface. The loading has a logarithmic singularity at the flap edges, which may be determined directly by the method of matched asymptotic expansions. Expressions are given for the singular flap loading for various flap hinge line and side edge geometries, both for steady and unsteady flap deflection. The regular part of the flap loading must be obtained by inverting the lifting-surface-theory integral equation relating the pressure and the downwash on the wing; procedures are described to accomplish this for a general wing and flap geometry. The method is applied to several example wings, and the results are compared with experimental data. Theory and test correlate well.

INTRODUCTION

Methods have been developed (e.g., refs. 1 and 2) for the application of lifting-surface theory to wings of various configurations: planar and nonplanar wings, one wing or several, and steady and unsteady flow. These methods, however, have not been able to accurately handle a wing with a trailing-edge flap. The lifting-surface-theory integral equation relating the pressure to the downwash at the wing is inverted by assuming the loading may be represented by a linear combination of suitable preselected pressure functions. Because of the large amount of numerical computation involved, it is important that only a few modes be used to give the loading accurately, and this is possible only if the preselected pressure functions match the true loading as closely as possible. The wing with a trailing-edge flap has a logarithmic singularity in the pressure at the flap hinge line and side edges, and it is the difficulty in accurately representing this singular behavior by the usual loading functions that has prevented the practical application of lifting-surface theory to such wings.

Landahl (ref. 3) has shown that with the aid of the method of matched asymptotic expansions the singular loading behavior near the flap edges can be obtained from simple steady flow problems in two and three dimensions. The singular part of the loading is not influenced by boundary conditions because of the presence of the other edges of the wing or flap. Consequently, the strength of the singularity at the flap edge is determined uniquely by the flap deflection and motion. Thus the pressure loading due to the flap may be written as the sum of a known singular part and an unknown regular part. The regular part must still be obtained by inverting the

lifting-surface-theory integral equation. However, the regular part may now be accurately represented by pressure modes of the usual type, and the solution for these follows the standard techniques of lifting-surface theory.

Landahl only gives the singular part of the pressure distribution for a few flap edge geometries. Some recent works (refs. 4 and 5) have considered the use of the singular flap pressure mode in lifting-surface theory, but have not carried the results far enough to obtain actual flap-induced loadings. This report gathers the results of lifting-surface theory and the flap pressure modes, extending them where necessary, to present a procedure that will allow researchers to use the ideas and techniques to obtain the loading on a wing with a trailing-edge flap. The principal idea is the use of the known singular flap pressure mode (Landahl) in the kernel function approach to lifting-surface theory. Much attention is given to the details of the actual numerical procedures involved, since the numerical difficulties are the primary obstacle between the knowledge of the flap pressure mode and the solution for the wing loading. The first section outlines one method for solving the lifting-surface-theory integral equation; the next section extends this method to include a wing with a flap or control surface. Then expressions are given that may be used to construct the singular flap pressure function for any wing and flap geometry. Finally the method presented is applied to several wings and the results compared with some experimental data.

OUTLINE OF LIFTING–SURFACE THEORY

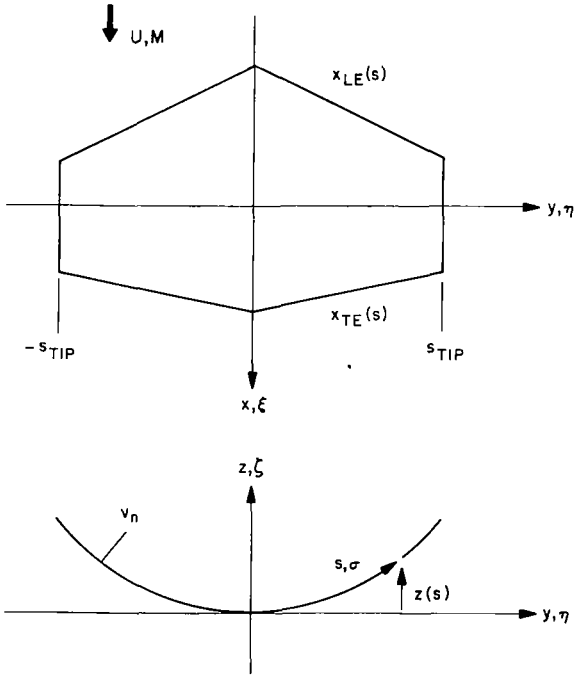

Figure 1.- Geometry of the wing surface.

The techniques of linear, potential aerodynamics may be used to relate the differential pressure on a thin wing surface to the downwash at the wing by an integral equation of the form

$$\frac{\overline{v}_n(x, s, \omega)}{U} = \iint_{\substack{\text{wing} \\ \text{surface}}} -\frac{\overline{\Delta p}(\xi,\sigma)}{\rho U^2} K(x - \xi, s, \sigma, \omega, M)\, d\xi\, d\sigma \qquad (1)$$

The wing (fig. 1) may consist, in general, of several nonplanar wing surfaces, although for simplicity of notation only one wing will be considered here. The linear problem replaces each thin wing by a surface of zero thickness; in general, each surface is a cylinder with generators parallel to the free-stream velocity U (the x axis). The pressure due to the wing thickness is a direct problem, which may be separated from the lifting problem, and is not considered here. The unsteady problem only considers sinusoidal time variation of the

velocity and pressure, so a factor $e^{i\omega t}$ has been suppressed from the integral equation. The downwash due to the external flow, normal to the wing surface, is $v_n = \bar{v}_n e^{i\omega t}$. The differential pressure on the wing surface, in the lifting direction, is $-\Delta p = -\overline{\Delta p} e^{i\omega t}$. The kernel function K is the downwash at the point (x,s) due to the pressure at the point (ξ,σ). Since the downwash is the known quantity and the pressure the unknown, this is an indirect problem; the inversion of the integral equation for the pressure is the primary difficulty of lifting-surface theory, and several methods and variations of methods have been developed to overcome it. A derivation and further discussion of the integral equation and the kernel may be found, for example, in references 1, 2, and 6.

The method of solving the integral equation to be used here follows closely that detailed in reference 1. The wing surface is normalized by transforming from the variables (ξ,σ) to the variables (θ,λ):

$$\xi = \bar{x}(\sigma) + b(\sigma)\cos\theta \tag{2}$$

$$\sigma = s_{TIP}\lambda \tag{3}$$

where

$$\bar{x}(\sigma) = \frac{1}{2}\left[x_{TE}(\sigma) + x_{LE}(\sigma)\right] \tag{4}$$

$$b(\sigma) = \frac{1}{2}\left[x_{TE}(\sigma) - x_{LE}(\sigma)\right] \tag{5}$$

The pressure is expanded as a series of the form

$$-\frac{\overline{\Delta p}(\theta,\lambda)}{\rho U^2} = \sum_{m=0}^{N_1}\sum_{n=0}^{N_2}\frac{a_{nm}g_m(\lambda)f_n(\theta)}{b(\lambda)} \tag{6}$$

where the chordwise and spanwise pressure modes are typically of the form (for a symmetrical wing and downwash distribution)

$$f_n(\theta) = \begin{cases} \tan\left(\frac{\theta}{2}\right) & n = 0 \\ \sin n\theta & n \geqslant 1 \end{cases} \tag{7}$$

$$g_m(\lambda) = \lambda^{2m}\sqrt{1-\lambda^2} \tag{8}$$

These modes have the proper behavior near the edges of the wing; for typical downwash distributions and wing planforms, only the first few modes are required to describe the pressure distribution adequately. If only a finite number of pressure modes are considered and the integral

equation is satisfied only at a finite number of collocation points (x_i,s_j), the integral equation is converted to a set of simultaneous linear algebraic equations

$$\frac{\bar{v}_n(x_i,s_j)}{U} = \sum_n \sum_m a_{nm}(I_{nm})_{ij} \tag{9}$$

The collocation points are distributed over the wing surface by a uniform rectangular matrix in the (ϕ,l) system

$$x_i = \bar{x} + b\cos\phi_i, \quad \phi_i = \left(i - \frac{1}{2}\right)\Delta\phi, \quad i = 1, 2, \ldots, N_3 \tag{10}$$

$$s_j = s_{TIP} l_j, \quad l_j = j\Delta l, \quad j = 1, 2, \ldots, N_4 \tag{11}$$

where

$$\Delta\phi = \frac{2\pi}{2N_3 + 1} \tag{12}$$

$$\Delta l = \frac{1}{N_4 + 1} \tag{13}$$

The number of collocation points is usually taken larger than the number of pressure modes, and the system of equations is inverted in a least squares sense for a given v_n to find a_{nm}. The pressure distribution may then be integrated to find the forces acting on the wing (e.g., the section lift and moment) and the total wing lift and moment.

The coefficients of the algebraic equations, $(I_{nm})_{ij}$, are integrals over the wing surface of the pressure modes times the kernel function; they are the downwash at the collocation point (x_i,s_j) due to the pressure mode a_{nm}. These integrals must be evaluated numerically, and with some care since the kernel function is singular as the integration point approaches the collocation point. The kernel function may be written as

$$K = \frac{1}{r_1^2}\,\bar{K} \tag{14}$$

$$r_1^2 = (y - \eta)^2 + (z - \zeta)^2 \tag{15}$$

where $\bar{K}$ has no spanwise singularity; at the spanwise station of the collocation point ($r_1 = 0$) $\bar{K}$ does have a chordwise discontinuity, of magnitude 2, at the collocation point. Thus the equation coefficients are

$$(I_{nm})_{ij} = \frac{s_{TIP}}{4\pi}\int_{-1}^{1} \frac{g_m(\lambda)}{r_1^2}\left[\int_0^{\pi} \bar{K}(x_i - \xi, s_j, \sigma, \omega, M) f_n(\theta)\sin\theta\, d\theta\right] d\lambda \tag{16}$$

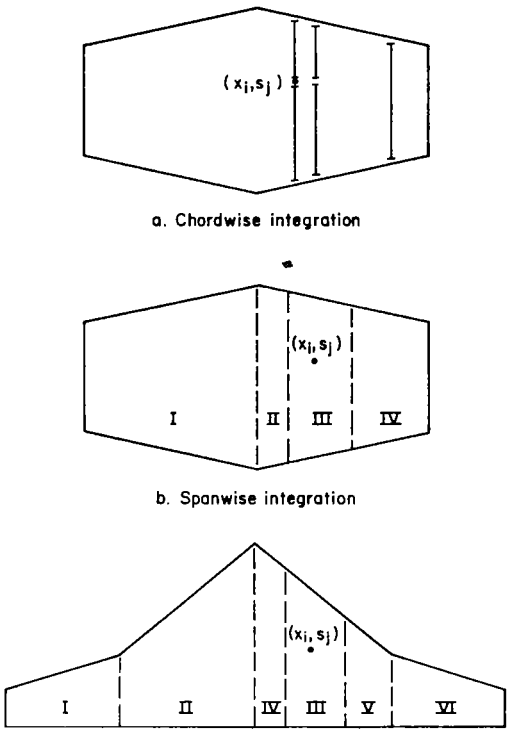

Figure 2.- Numerical integration of pressure modes over wing surface.

The chordwise integration is performed first. If the spanwise station is at or close to the collocation point, the discontinuity in $\overline{K}$ requires that the integration be broken into two intervals, one ahead of and one behind the collocation point (fig. 2(a)). Quantitatively the criterion is that two intervals are used if $r_1^2 < 0.1$ and one interval if $r_1^2 > 0.1$. The integral over each interval is evaluated numerically by a gaussian quadrature over θ. Next the spanwise integration is performed. The spanwise integration is broken into four intervals (fig. 2(b)). It is broken at the wing centerline to allow for a discontinuity there in the wing sweep (a kink). Region III in figure 2(b) is a narrow strip about the collocation point of width 2ϵ, where ϵ is taken as 30 percent of the separation between the collocation points: $\epsilon = 0.3\,\Delta l$. The integrals in regions I, II, and IV are well behaved and are readily evaluated by gaussian quadratures over λ_{-2}. The integrand in region III includes the spanwise r_1^{-2} singularity; the integral over this interval is a singular integral of Mangler's type. A technique for evaluating this integral is detailed in reference 1; it involves approximating the regular part of the integrand by a seven-point Lagrange interpolation polynomial, and evaluating the integral of the product of r_1^{-2} with the polynomial using Mangler's formulas.

For wings with discontinuities in sweep angle, the spanwise integral should also be broken at each kink (fig. 2(c)). In general, the technique of integration is to divide the wing surface into panels, in the interior of which the integrand has entirely regular behavior. All singularities and discontinuities, due either to the kernel function or to the wing planform shape, are kept at the edges of the panels. The integration over each panel (with the exception of the panel with the r_1^{-2} spanwise singularity, which is handled separately as outlined above) is performed numerically by a gaussian quadrature, which has the property of concentrating the integration points near the ends of the interval while avoiding the integrand exactly at the end points. Moreover, there are the same number of quadrature points in each panel. Therefore as the planform becomes more complex the total number of integration points automatically increases because of the increase in number of panels.

The collocation points should be distributed separately in each wing panel between planform discontinuities, to avoid putting points at or near the kinks. The pressure distribution will be changing most rapidly near such kinks (to put a collocation point there would emphasize this rapid change) leading to a poor representation of the pressure if few collocation points and pressure modes are used. These techniques of numerical integration and placement of the collocation points will also be followed when the trailing-edge flap is introduced.

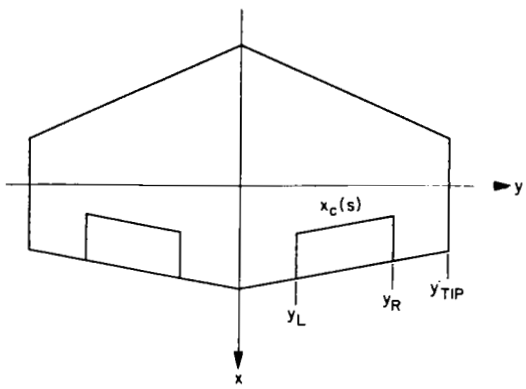

Figure 3.- Geometry of wing with trailing-edge flap.

The integral equation between the downwash and pressure (eq. (1)) is still the governing equation for a wing with a trailing-edge flap. A typical wing geometry is shown in figure 3; only a planar wing is considered for the flap case, so $s = y$. The flap hinge line is given by

$$x_c = \bar{x} + b[1 - 2c_f(s)]$$

$$= \bar{x} + b\cos\phi_c \qquad (17)$$

where $c_f(s)$ is the ratio of the local flap chord to the local wing chord. The flap pressure functions (to be described later) require that x_c be continuously defined also in wing panels without a flap.

The downwash due to a downward flap deflection $\delta_f = \bar{\delta}_f e^{i\omega t}$ is

$$\frac{\bar{v}_n}{U} = \begin{cases} -\bar{\delta}_f[1 + ik(x - x_c)] & \text{on the flap surface} \\ 0 & \text{off the flap surface} \end{cases} \qquad (18)$$

where the wave number $k = \omega/U$. Only the downwash due to the flap is considered. The downwash due to wing angle of attack, camber, heaving, and other wing motions does not involve the flap in any way; when the loading due to this downwash has been obtained, by the usual methods, it may be linearly combined with the flap loading to give the pressure on the wing due to its complete motion.

The pressure is again expanded as a sum of modes. With the trailing-edge flap, the pressure distribution has a logarithmic singularity at the hinge line and at the flap side edges; however, this singular part of the pressure distribution may be obtained directly by the methods of matched asymptotic expansions (ref. 2), and the remainder is a regular distribution that may be adequately represented by a series of the usual form. Thus the pressure loading induced by the trailing-edge flap is written as

$$\frac{-\overline{\Delta p}(\theta,\lambda)}{\rho U^2} = \frac{\sum_n \sum_m a_{nm} g_m(\lambda) f_n(\theta)}{b(\lambda)} + \bar{\delta}_f g_f(\theta,\lambda) \qquad (19)$$

where g_m and f_n are given as before by equations (7) and (8), and $g_f(\theta,\lambda)$ is the flap pressure mode for the specific flap and wing geometry considered. Expressions for g_f will be given below.

The collocation points (x_i, s_j) are distributed in a rectangular matrix in the (ϕ, l) coordinate system. On wing panels without the trailing-edge flap, the chordwise distribution is still given by equation (10). On panels with the flap, half the points are ahead of the hinge line and half behind;

the distribution in each interval being uniform in ϕ. Again the wing leading edge and trailing edge and the flap hinge line are avoided in distributing the points. The spanwise distribution of the collocation points is equally apportioned among each wing panel, with and without a flap, avoiding the edges of panels (which are at the flap edges, the wing tips, or kinks in the wing planform); the distribution in each panel is uniform in l.

When only a finite number of pressure modes and collocation points are considered, and the pressure expansion (eq. (19)) is substituted into the integral equation (eq. (1)), a system of linear algebraic equations results

$$\frac{\bar{v}_n^*(x_i,s_j)}{U} = \sum_n \sum_m a_{nm}(I_{nm})_{ij} \tag{20}$$

Here since the pressure mode g_f is known, it has been moved to the left side of the equation to give an effective downwash $\bar{v}_n^*$

$$\frac{\bar{v}_n^*}{U} = \frac{\bar{v}_n}{U} - \bar{\delta}_f(I_f)_{ij} \tag{21}$$

Equation (20) is of exactly the same form as equation (9), and may be inverted for the pressure coefficients a_{nm} when the effective downwash $\bar{v}_n^*$ has been calculated. The total pressure distribution, including both the singular mode g_f and the regular modes a_{nm}, may then be integrated to find the forces acting on the wing.

The coefficients $(I_{nm})_{ij}$ are still given by equation (16). The integrand is a product of the regular pressure mode and the kernel function; since these do not involve the flap, the numerical evaluation of $(I_{nm})_{ij}$ proceeds exactly as described above for the wing without the flap.

The equivalent downwash involves the integral over the wing surface of the flap pressure times the kernel function

$$(I_f)_{ij} = \frac{{}^sTIP}{4\pi} \int_{-1}^{1} \frac{b(\lambda)}{r_1^2} \left[\int_0^{\pi} \bar{K}(x_i - \xi, s_j, \sigma, \omega, M) g_f(\theta,\lambda) \sin\theta \, d\theta \right] d\lambda \tag{22}$$

where $(I_f)_{ij}$ is the downwash at the collocation point (x_i,s_j) due to the flap pressure mode. The numerical evaluation of $(I_f)_{ij}$ follows that of $(I_{nm})_{ij}$, with the integrals broken into more intervals to handle the singularities of the pressure function g_f. The chordwise integration, in addition to being broken at the collocation point, is broken at the flap hinge if the spanwise station includes the flap or is near the edge of the flap (fig. 4(a)); the latter criterion is quantitatively that $r_s^2 < 0.1$ where r_s is the distance to the flap side edge. The integral over each interval (there being one, two, or three intervals now) is evaluated by a gaussian quadrature over θ. The spanwise integration, in addition to being broken at each kink in the wing planform and a distance ϵ either side of the

collocation point, is broken at each flap side edge (fig. 4(b)). The integral over each wing panel (except for the strip including the collocation point, which is handled separately again, as outlined above) is evaluated numerically by a gaussian quadrature over λ.

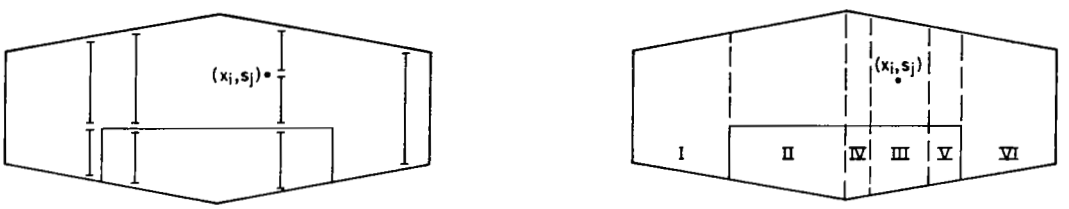

a. Chordwise integration

b. Spanwise integration

Figure 4.- Numerical integration of flap pressure mode.

THE FLAP PRESSURE MODE

Formulas are presented here for g_f, the singular part of the pressure due to the trailing-edge flap. A logarithmic singularity at the hinge line and the side edges is caused by the flow turning instantaneously through a finite angle. The singularity is a local phenomenon, independent of the presence of the edges of the wing or other flap edges; consequently, the methods of matched asymptotic expansions may be applied to solve for the pressure singularity directly. Landahl (ref. 3) has used this technique for several configurations; his results will be consolidated and in some cases extended here. Expressions for $-\overline{\Delta p}/\rho u^2$ due to unit $\overline{\delta}_f$ are given for several edge configurations; when combined appropriately for a particular flap geometry and modified to have correct behavior at the wing edges, these expressions give the flap pressure mode g_f. Quantities that enter into these expressions are

$$\beta^2 = 1 - M^2 \tag{23}$$

$$\tan \Lambda = \frac{dx_c}{dy} \tag{24}$$

$$\left(\frac{\beta_N}{\cos \Lambda}\right)^2 = \beta^2 + \tan^2 \Lambda \tag{25}$$

where β is the Prandtl-Glauert compressibility factor.

The pressure due to a flap hinge on a two-dimensional airfoil, or a hinge line on a wing far from the flap side edges is

$$P_{2D} = -\frac{1}{\pi\beta_N/\cos \Lambda} \, ln(x - x_c)^2 \tag{26}$$

Landahl considers only an unswept hinge line at the flap corner; he finds the corner pressure function (eq. (27) of ref. 3) from a line of sources distributed along the flap hinge line. This result may be extended to obtain the pressure due to a swept hinge corner by matching the pressure due to a line of sources distributed along a straight line at an angle $\Lambda(y_L)$ to the pressure due to a swept hinge line (P_{2D}). The pressure due to a left corner plus the flap hinge line is then

$$P_{Lh} = -\frac{1}{\pi\beta_N/\cos\Lambda}\, ln\left\{\left[(x - x_c)^2 + 2\tan\Lambda(y - y_L)(x - x_c) + \frac{\beta_N^2}{\cos^2\Lambda}(y - y_L)^2\right]^{1/2}\right.$$

$$\left. - (x - x_c)\frac{\tan\Lambda}{\beta_N/\cos\Lambda} - (y - y_L)\frac{\beta_N}{\cos\Lambda}\right\} \tag{27}$$

Similarly the pressure due to a right corner plus the flap hinge line is

$$P_{Rh} = -\frac{1}{\pi\beta_N/\cos\Lambda}\, ln\left\{\left[(x - x_c)^2 + 2\tan\Lambda(y - y_R)(x - x_c) + \frac{\beta_N^2}{\cos^2\Lambda}(y - y_R)^2\right]^{1/2}\right.$$

$$\left. + (x - x_c)\frac{\tan\Lambda}{\beta_N/\cos\Lambda} + (y - y_R)\frac{\beta_N}{\cos\Lambda}\right\} \tag{28}$$

where y_L is the location of the left corner and y_R is the location of the right corner; $\tan\Lambda$ must have a continuous definition beyond the flap corner.

The pressure due to a flap hinge line with left and right corners may be found by adding P_{Lh} and P_{Rh} and subtracting their common part

$$P_h(y_L, y_R) = P_{Lh} + P_{Rh} - P_{2D} \tag{29}$$

For a flap with a kink in the hinge line at y_s (i.e., $\tan\Lambda = dx_c/dy$ discontinuous there) the pressure is obtained as a sum of terms for each continuous segment

$$P_{kh}(y_L, y_R, y_s) = P_h(y_L, y_s) + P_h(y_s, y_R) \tag{30}$$

where $\tan\Lambda$ must have a continuous definition beyond the end points of each term.

Landahl only gives the pressure for the flap side edge with one end, at the hinge line. The pressure including the effect of ending the side edge at the wing trailing edge may be found by adding the terms due to the two ends and subtracting their common part. The result for a left side edge at y_s is

$$P_{Lse} = \frac{1}{\pi}[2ik - k^2(x - x_c)](y - y_s)\left\{ln\left[\sqrt{(x - x_c)^2 + \beta^2(y - y_s)^2} - (x - x_c)\right]\right.$$

$$\left. + ln\left[\sqrt{(x - x_{TE})^2 + \beta^2(y - y_s)^2} + (x - x_{TE})\right] - ln(y - y_s)^2\right\} \tag{31}$$

Similarly, for a right side edge at y_s

$$P_{Rse} = -P_{Lse} \tag{32}$$

It should be noted that the wing tip is not a side edge; a flap side edge is where the flap surface joins the wing surface.

The expressions for the pressure due to the flap hinge line and side edges must be modified to have the correct behavior at the wing edges. This is accomplished by multiplying the uncorrected pressure functions by factors that have the value unity at the flap boundary and go to zero at the wing edges with the square root of the distance from the edge. The hinge line pressure is multiplied by chordwise and spanwise factors:

$$P_h^c = f_c(x) f_s(y) P_h \tag{33}$$

The chordwise factor is

$$f_c = \begin{cases} \sqrt{\dfrac{x - x_{LE}}{x_c - x_{LE}}} & \text{for } x < x_c \\ \sqrt{\dfrac{x_{TE} - x}{x_{TE} - x_c}} & \text{for } x > x_c \end{cases} \tag{34}$$

The spanwise factor depends on the wing geometry and flap geometry; several cases are considered below.

1. For a wing with pointed or rounded tips

$$f_s = 1 \tag{35}$$

2. For a wing with square tips, and a full span flap

$$f_s = \sqrt{\frac{y_{TIP}^2 - y^2}{y_{TIP}^2 - y^2 + (x - x_c)^2}} \tag{36}$$

3. For a wing with square tips, and a part span flap

$$f_s = \begin{cases} \sqrt{1 - [(y_L - y)/(y_L + y_{TIP})]^2} & -y_{TIP} < y < y_L \\ 1 & y_L < y < y_R \\ \sqrt{1 - [(y - y_R)/(y_{TIP} - y_R)]^2} & y_e < y < y_{TIP} \end{cases} \tag{37}$$

4. Other configurations (e.g., a flap, with an inboard edge, extending to the tip) may be handled by combining the above kinds of factors.

The corrected side-edge pressure function is

$$P^{c}_{Lse} = f_c(x) f_s(y) P_{Lse} \tag{38}$$

where the spanwise factor is

$$f_s = \begin{cases} \sqrt{\dfrac{y_{TIP} + y}{y_{TIP} + y_s}} & \text{for } y < y_s \\ \sqrt{\dfrac{y_{TIP} - y}{y_{TIP} - y_s}} & \text{for } y > y_s \end{cases} \tag{39}$$

and the chordwise factor is

$$f_c = \sqrt{\frac{(x - x_{LE})(x_{TE} - x)}{(x - x_{LE})(x_{TE} - x) + (y - y_s)^2}} \tag{40}$$

The construction of P^{c}_{Rse} is similar.

The flap pressure mode g_f is obtained by adding the appropriate corrected pressure function for each flap hinge line and each flap side edge. A flap hinge line with a kink is effectively two separate hinge lines, each with two corners, but with no side edge at the kink. A better representation is obtained if for a symmetrical wing, the flap pressure function is not continued from one side to the other (i.e., on each side of the wing centerline only the pressure due to the flap on that side is used). The pressure due to the flap on the other side is a regular part, and convergence is improved if it is dropped. Since the wing is symmetrical, the pressures on the two sides do match at the center. This consideration for the kinked flap does not affect the flap pressure function for a flap that is continuous (and not kinked) across the centerline.

An antisymmetrical flap configuration (i.e., ailerons) may also be handled simply by using antisymmetrical span loading functions g_m and constructing an antisymmetrical flap pressure mode.

EXAMPLES AND COMPARISONS WITH EXPERIMENT

Some results of applying the method described above are presented here for the use of lifting-surface theory with a trailing-edge flap. It was found that three to four chordwise pressure modes (f_n) and three to four spanwise modes (g_m) gave an adequate representation of the regular part of the pressure distribution; the number of modes required will vary with the wing and flap geometry, however, and should be determined for each new case considered.

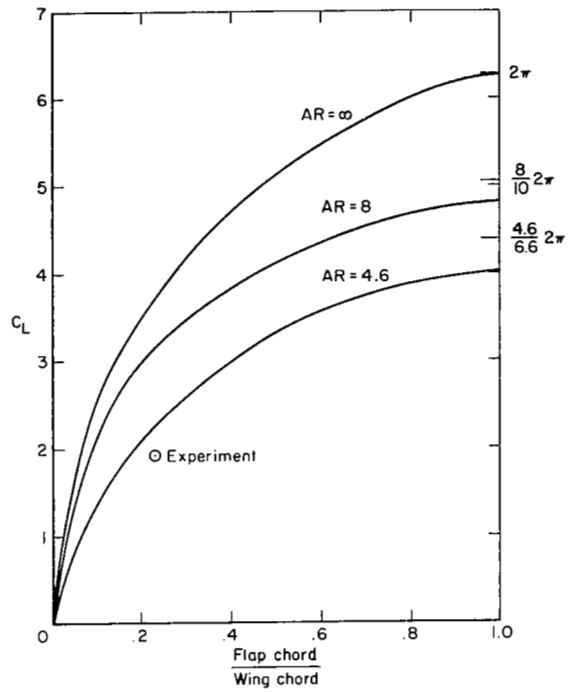

Figure 5.- Wing lift coefficient calculated by lifting-surface theory, for a rectangular wing with trailing-edge flap; the experimental point is for a wing with aspect ratio 4.6 (ref. 7).

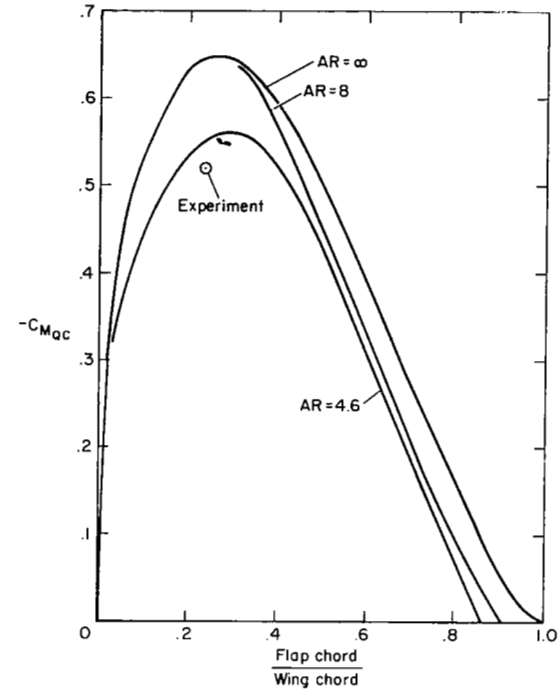

Figure 6.- Wing moment coefficient (about the quarter chord) calculated by lifting-surface theory, for a rectangular wing with a trailing-edge flap; the experimental point is for a wing with aspect ratio 4.6 (ref. 7).

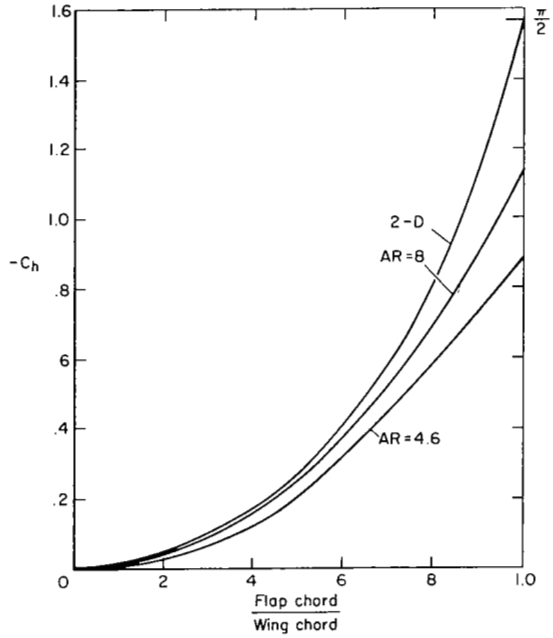

Figure 7.- Wing hinge moment coefficient calculated by lifting-surface theory, for a rectangular wing with a trailing-edge flap.

Figures 5, 6, and 7 show the variation of lift, pitching moment, and hinge-moment coefficients with flap chord to wing chord ratio for a rectangular wing with full-span trailing edge and steady, unit flap deflection ($\delta_f = 1$, $k = 0$). The two-dimensional airfoil results (Theodorsen theory) are compared with the lifting-surface-theory results for wings of aspect ratios of 8 and 4.6. Also shown are experimental points for a wing of 4.6 aspect ratio with a 23 percent chord trailing-edge flap (ref. 7). The lift coefficient (fig. 5) shows a substantial effect of aspect ratio; the lifting line theory result, $C_L = 2\pi AR/(AR + 2)$, for a 100 percent chord flap is also indicated in the figure.

Data are given in reference 8 for the loading on an aspect ratio 2, triangular wing with a full-span trailing-edge flap (constant flap chord, 10.7 percent of the wing root chord) deflected 9.5° (nominal 10°). The wing C_L, C_m, and C_h from the experiment and calculated by the

lifting-surface theory are compared below.

Coefficient	Experiment	Theory
C_L	0.23	0.228
C_m	-.08	-.090
C_h	-.11	-.114

Figure 8 compares the experimental and theoretical section lift coefficient; the lift coefficient is based on the local chord, which goes to zero at the tip faster than the actual loading, resulting in the large lift coefficients at the tip. Figure 9 compares the experimental and theoretical section center of pressure location, expressed as a fraction of the local chord. The differences between the experimental and theoretical values for the loading on this wing are well within the accuracy of the experimental data.

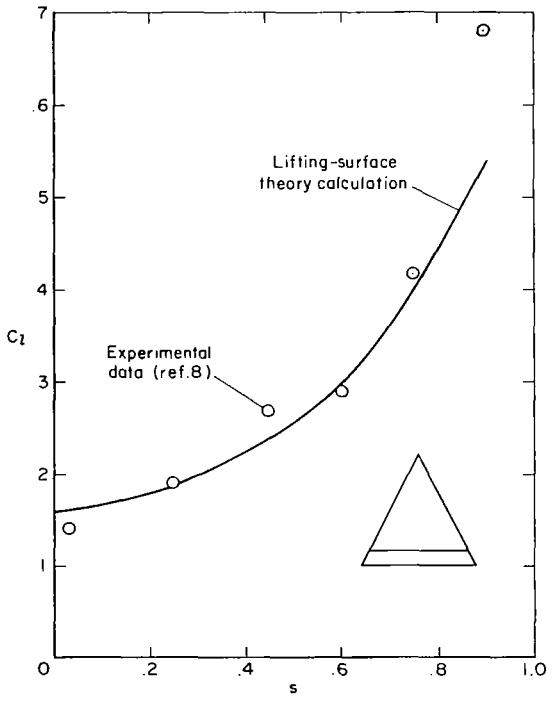

Figure 8.- Section lift coefficient on triangular wing with full span trailing-edge flap; $\delta_f = 9.5°$, flap chord = 10.7 percent wing root chord.

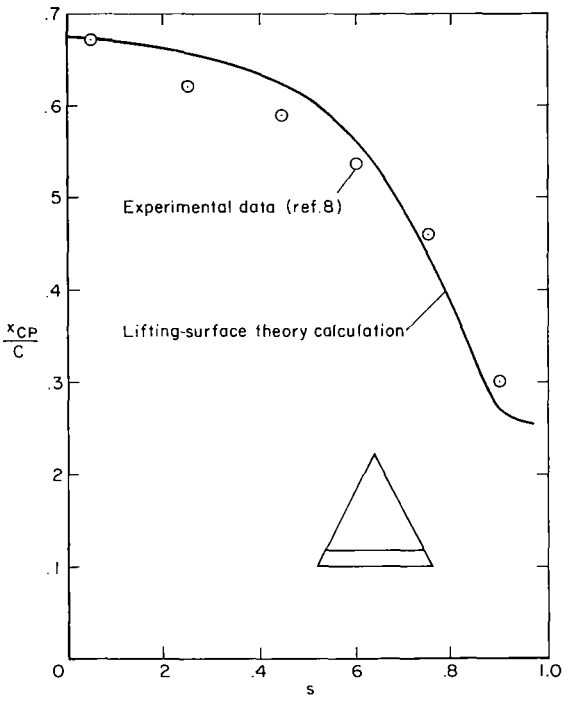

Figure 9.- Section center of pressure on a triangular wing with full span trailing-edge flap; $\delta_f = 9.5°$, flap chord = 10.7 percent wing root chord.

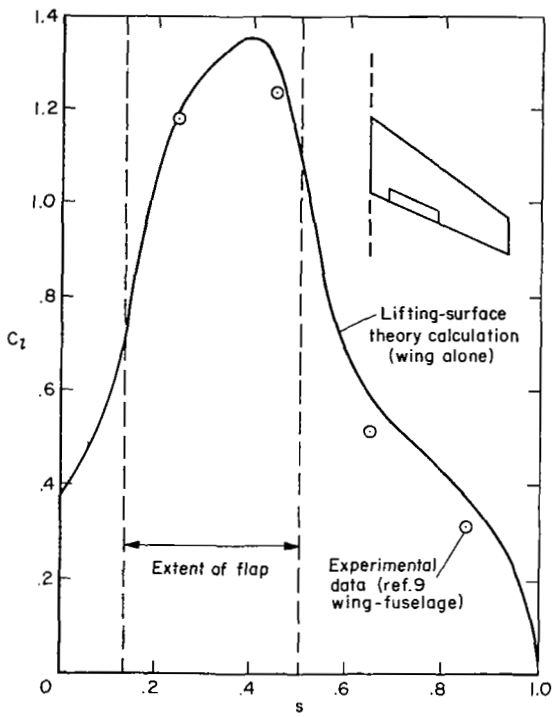

Figure 10.- Section lift coefficient on a swept wing with a partial span flap; $\delta_f = 52.1°$ (area suction on flap leading edge).

A final wing was considered, one that included both a partial span flap and sweep of the flap hinge line (ref. 9). The wing had an aspect ratio of 4.785, a taper ratio of 0.513, and 35° sweep of the quarter chord line. The flap extended from $y_L = 0.135\, y_{TIP}$ to $y_R = 0.5\, y_{TIP}$, with a constant chord, 14.5 percent of the wing root chord. The flap deflection was 52.1°, with area suction on the flap leading edge to maintain attached flow. Figure 10 compares the experimental and theoretical section lift coefficient for this wing, showing good agreement.

The limited examples and comparison with experiment presented in this section demonstrate the applicability of the method described above for the use of lifting-surface theory on a wing with a trailing-edge flap. The details of the numerical procedures and the construction of the flap pressure function depend heavily on the specific wing and flap geometry considered. Therefore it is not possible to give a single general flap pressure mode and solution procedure that will handle all possible cases. The formulas and methods presented here, however, should be sufficient to allow the practical use of lifting-surface theory for the calculation of the loading on any given wing and flap configuration.

Ames Research Center
National Aeronautics and Space Administration
and
U. S. Army Air Mobility R & D Laboratory
Moffett Field, Calif., 94035, Nov. 8, 1971

REFERENCES

1. Watkins, Charles E.; Woolston, Donald S.; and Cunningham, Herbert J.: A Systematic Kernel Function Procedure for Determining Aerodynamic Forces on Oscillating or Steady Finite Wings at Subsonic Speeds. NASA TR R-48, 1959.

2. Ashley, Holt; Widnall, Sheila E.; and Landahl, Marten T.: New Directions in Lifting Surface Theory. AIAA J., vol. 3, no. 1, Jan. 1965, pp. 3-16.

3. Landahl, M.: Pressure-Loading Functions for Oscillating Wings With Control Surfaces. AIAA J., vol. 6, no. 2, Feb. 1968, pp. 345-348.

4. Ashley, H.; and Rowe, W. S.: On the Unsteady Aerodynamic Loading of Wings With Control Surfaces. Z. Flugwiss., vol. 18, no. 9/10, 1970, pp. 321-330.

5. Crespo, Alfredo N.; and Cunningham, Herbert J.: Development of Three-Dimensional Pressure-Distribution Functions for Lifting Surfaces With Trailing-Edge Controls Based on the Integral Equation for Subsonic Flow. NASA TN D-5419, 1969.

6. Watkins, Charles E.; Runyan, Henry L.; and Woolston, Donald S.: The Kernel Function of the Integral Equation Relating the Lift and Downwash Distributions of Oscillating Finite Wings in Subsonic Flow. NACA TR 1234, 1955.

7. Carter, Arthur, W.: Pressure Distributions on a Wing Having NACA 4415 Airfoil Sections With Trailing-Edge Flaps at 0° and 40°. NASA TM X-2225, 1971.

8. Graham, David: Chordwise and Spanwise Loadings Measured at Low Speeds on a Large Triangular Wing Having an Aspect Ratio of 2 and a Thin, Subsonic-Type Airfoil Section. NACA RM A50A04a, 1950.

9. Cook, Woodrow L.; Holzhauser, Curt A.; and Kelly, Mark W.: The Use of Area Suction for the Purpose of Improving Trailing-Edge Flap Effectiveness on a 35° Sweptback Wing. NACA RM A53E06, 1953.

NASA-Langley, 1972 — 1 A-4084